

Description of complex strain-optical coefficient by the Fractional Standard Solid Model

Nicole Heymans
 Université Libre de Bruxelles
 Physique des Matériaux de Synthèse 259
 BE 1050 Bruxelles
 BELGIUM
 Nicole.Heymans@ulb.ac.be

Abstract – The Fractional Standard Solid Model for viscoelasticity is recalled. In association with an existing model for birefringence in polymers, it allows interpretation of literature data on dynamic birefringence in polycarbonate in the glass transition range. This model, which does not require validity of the frequency-temperature superposition principle, is compared with Inoue et al's decomposition into rubbery and glassy components of relaxation functions.

I. INTRODUCTION

The complex strain-optical coefficient (SNOC) of amorphous polymers in the glass transition region within the linear viscoelastic limit has been interpreted by Inoue, Osaki et al in terms of a modified stress-optical law involving at least two additive components of stress or modulus (one glassy and one rubbery) [1-4]. Each component is a function of temperature and frequency. However, the assumption of stress additivity, which amounts to use of a generalized Maxwell model, leads to unexpected behaviour in creep and recovery, because the several Maxwell elements cannot recover independently if total stress is maintained constant [5].

Alternative models have been introduced recently, based on descriptions of viscoelasticity using non-integer order stress and strain derivatives. These descriptions are particularly well-suited to describing steady-state dynamic behaviour and can be applied to materials which violate time-temperature superposition [6-8]. A novel formulation of the dynamic stress-optical law will be given here based on a Zener model incorporating a fractional viscoelastic element (spring-pot), or Fractional Standard Solid model. This leads to definition of two components of strain: a glassy elastic component and a transition component. For the latter component there are two contributions to stress: a viscoelastic spring-pot component, and a soft elastic component representing rubbery behaviour. In the small-strain linear viscoelastic limit this component is proportional to the corresponding stress.

In the glassy state birefringence arises mainly from changes in interatomic spacings and from distortion of repeat units. These may both be assumed proportional to stress. In the melt, birefringence arises from strain-dependent orientation of Kuhn segments and an identical strain-optical coefficient can be assumed for the rubbery elastic and spring-pot components.

Birefringence arising during deformation of amorphous polymers has been successfully described as a complex

interaction between distortion and orientation [9-10]. However, in the linear viscoelastic limit, it may be assumed that these contributions are simply additive.

The resulting description of birefringence will be applied to literature data on polycarbonate.

II. DATA

The data that will be analysed in this paper are the dynamic strain-optical data of Hwang et al. [1], given on Figs. 1-4. Figs 1 and 2 give dynamic modulus, and Figs 3 and 4 give complex strain optical constant (SNOC).

Hwang et al [1] analysed the data by assuming additivity of two components (glassy and rubbery) of both modulus and birefringence. Under the additional assumption that the glassy and rubbery stress-optical constants are independent of frequency and temperature, they decompose modulus and strain-optical coefficient into their component functions E^*_R , E^*_G , O^*_R and O^*_G from the system:

$$E^* = E^*_R + E^*_G, \quad (1)$$

$$O^* = C_R E^*_R + C_G E^*_G, \quad (2)$$

where the stress-optical constants C_R and C_G are obtained from limiting behaviour at high and low temperatures respectively. Equations (1) and (2) expand into four linear equations in four unknowns, E'_R , E''_R , E'_G and E''_G , allowing the component functions to be obtained as a function of frequency at each temperature.

III. MODEL

A. The spring-pot and the Fractional Standard Model

The properties of a spring-pot have been fully discussed previously; only the essential properties are recalled here.

A spring-pot is defined as a rheological element having a complex modulus

$$E^* = K(i\omega)^\beta, \quad (3)$$

where K is consistency and $0 \leq \beta \leq 1$. Behaviour is Hookean elasticity when $\beta=0$ and Newtonian viscosity when $\beta=1$. The relaxation modulus and creep compliance are respectively

$$\sigma = \frac{K\varepsilon_0}{\Gamma(1-\beta)} t^{-\beta} \quad \text{and} \quad \varepsilon = \frac{\sigma_0}{K \Gamma(1+\beta)} t^\beta. \quad (4)$$

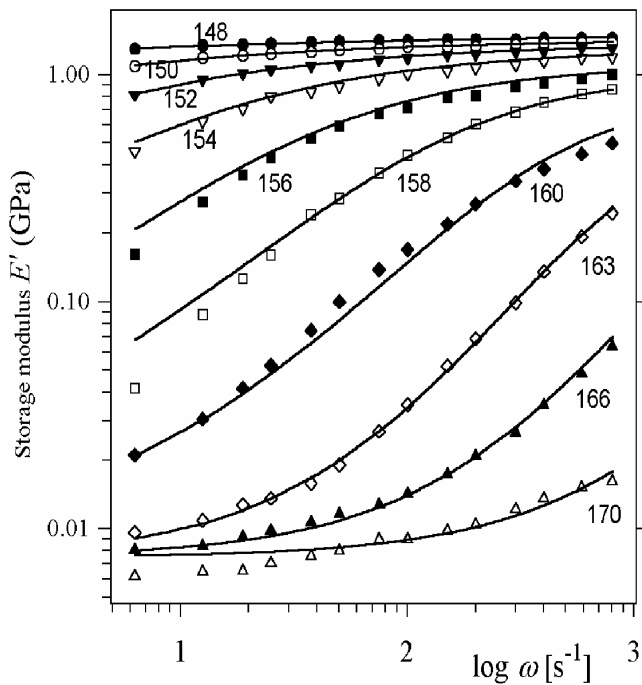


Fig. 1. Storage modulus of polycarbonate vs. angular frequency. Symbols: data from [1]. Lines: calculated from (5), parameters of table I. Numbers are temperature in °C.

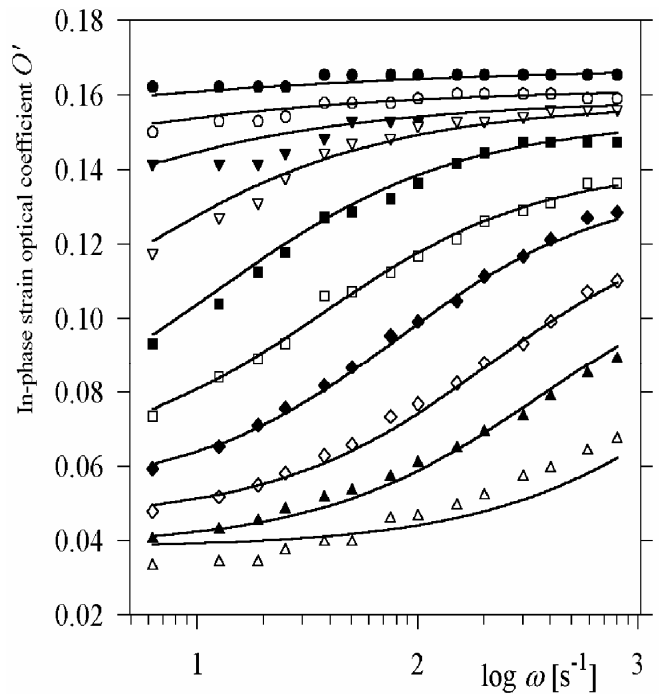


Fig. 3. In-phase SNOC of polycarbonate vs. angular frequency. Data from [1], symbols as Fig. 1. Curves calculated from (8), parameters of table II.

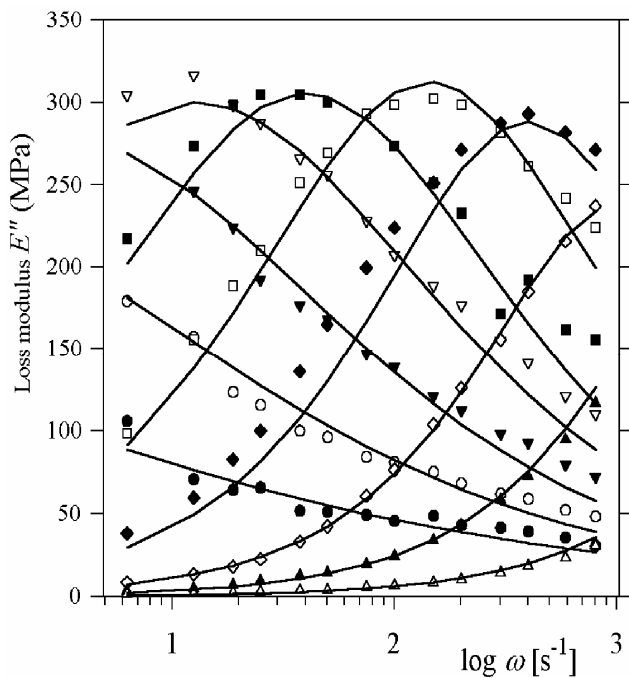


Fig. 2. Loss modulus of polycarbonate vs. angular frequency. Symbols and lines as Fig. 1.

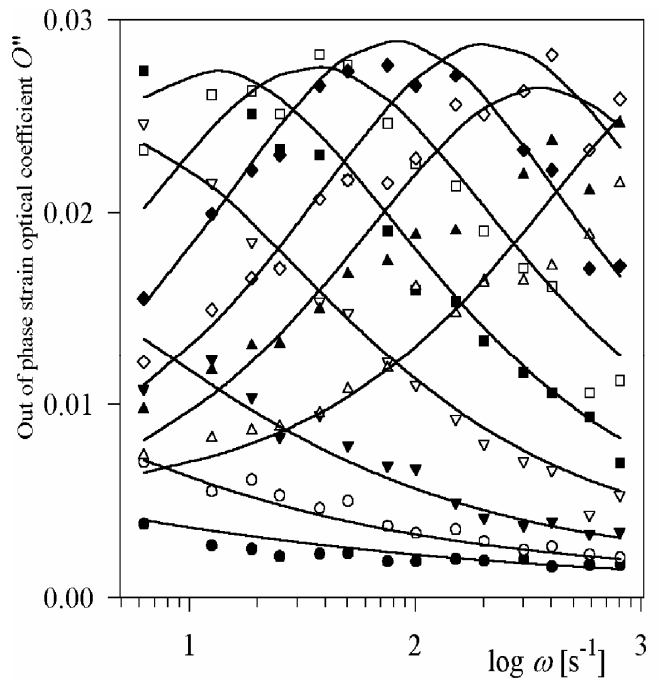


Fig. 4. Out of phase SNOC of polycarbonate vs. angular frequency. Symbols and lines as Fig. 3.

A spring-pot on its own is non standard: it has an infinite instantaneous modulus or vanishing instantaneous compliance. However, it can be associated with a series spring to obtain a standard Maxwell model for a viscoelastic fluid.

The simplest model able to describe a single viscoelastic transition such as the glass transition where long-term or low frequency behaviour is that of a (rubbery) solid, is the fractional Zener model or Fractional Standard Solid Model (FSSM) shown on Fig. 5. The complex modulus of this model is

$$E^* = \frac{E_0(E_1 + K(i\omega)^\beta)}{E_0 + E_1 + K(i\omega)^\beta} = \frac{E_r + E_u(i\omega\tau)^\beta}{1 + (i\omega\tau)^\beta}, \quad (5)$$

i.e. a Cole-Cole function, where E_r and E_u are relaxed and unrelaxed modulus respectively, and $(K/(E_0+E_1))^{1/\beta}$ is the time constant for modulus, denoted τ . Loss modulus is maximum when $\omega\tau=1$. When several neighbouring transitions occur, more elaborate models are required. However, the total number of adjustable parameters remains small: typically, 3 parameters per transition, plus one [7-8]. In this paper, the model will be applied to strain-optical behaviour of polycarbonate in the glass transition range. Because the highest secondary transition of polycarbonate (approx. -50°C) is far below the glass transition range (approx. 150°C), the simple fractional Zener model or FSSM of Fig. 5 will be applied here.

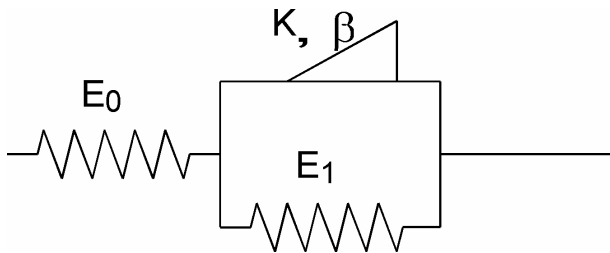


Fig. 5. Fractional Standard Solid Model (FSSM)

B. Relationship among stress, strain and birefringence

A description of development of birefringence during deformation of polymers has been given previously [9-11]. In this model, the anisotropy of the orienting element is assumed to depend on its orientation with respect to applied stress. For uniaxial applied stress, the element's anisotropy can be expanded in terms of even order Legendre polynomials or spherical harmonics:

$$\Delta n_e = \Delta n_{e0} + k_2 P_2 + \dots \quad (6)$$

where $P_2 = (3\cos^2 \theta - 1)/2$, θ is the angle between the local axis of the orienting element and the direction of applied stress, and k_2 depends on the distortional contribution to strain. The resulting global anisotropy is given by Equation (7), where dots represent terms arising from coefficients of higher-order Legendre polynomials in (6) and angular brackets denote averages over all orienting elements. In [10]

it was shown that higher order terms in (6) were expected to be vanishingly small, and that the fourth-order orientation average could also be omitted except at very high deformations.

$$\begin{aligned} \Delta n &= \langle \Delta n_e P_2 \rangle \\ &= \frac{k_2}{5} + \left(\Delta n_{e0} + \frac{2k_2}{7} + \dots \right) \langle P_2 \rangle + \left(\frac{18k_2}{35} + \dots \right) \langle P_4 \rangle + \dots \end{aligned} \quad (7)$$

Equation (7) shows that when accounting for both orientation and distortion of orienting elements, the two contributions to global anisotropy are not simply additive, but also give rise to the cross-term $k_2 \langle P_2 \rangle$. However, when applying this description to dynamic birefringence, i.e. in the linear range of viscoelasticity where strain and orientation are small, the cross-term which is of second order can be expected to vanish. The second-order orientation average $\langle P_2 \rangle$ depends on strain; however, the functional dependence will vary with temperature. Pseudo-affine and rubbery-elastic affine behaviour are expected respectively in the glassy and rubbery temperature ranges. A model interpolating between these two extremes was applied previously to orientation in the glassy range at high strains [11]. Such intermediate behaviour can also be expected at low strains in the glass-rubber transition range.

Finally, we can expect birefringence at low strains to be some linear combination of stress and strain; however, the coefficients in this combination are expected to be temperature dependent and cannot therefore be obtained simply from limiting behaviour at high and low temperatures. Nonetheless, it can be expected that the SNOG will also be given by a Cole-Cole expression similar to (5):

$$O^* = \frac{O_r + O_u(i\omega\tau)^{\beta_1}}{1 + (i\omega\tau)^{\beta_1}} \quad (8)$$

IV DISCUSSION

A. Glassy and rubbery relaxation functions

In the method described by Hwang et al [1], at each frequency and temperature, values for E^*_R and E^*_G are obtained from (1) and (2), which constitute a set of four linear equations. Frequency-temperature superposition is then applied to obtain master curves for E'_R , E''_R , E'_G and E''_G . Only the resulting master curves are given in [1]. The solution obtained by this method is unique; however unicity is not a proof of validity.

Firstly, how good is frequency-temperature superposability? Rather than looking at E' or E'' vs. angular frequency, validity or failure of superposability is far better revealed in a Cole-Cole plot (E'' vs E'). This plot is given on Fig. 6. If frequency-temperature superposition holds, data at all temperatures should fall on a single curve. This is clearly not the case. Hence an alternative method of data analysis is required, which does not rely on data reduction to master curves.

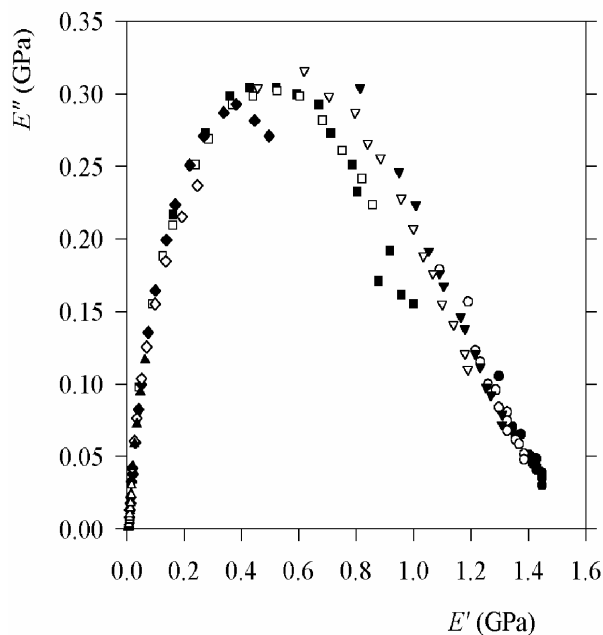


Fig. 6. Cole-Cole plot for complex modulus of polycarbonate in the glass transition range. Data and symbols identical to figs. 1 and 2.

Next, the behaviour of the component functions E_R^* and E_G^* is somewhat unexpected. E_R^* and E_G^* both display an asymmetric peak. Such peaks are frequently observed in polymer viscoelasticity. However, the usual occurrence is that the high temperature or low frequency side is steeper than the low temperature, high frequency side. This is indeed the case for E_G^* , and indeed the Cole-Cole plot of Fig. 6 also shows this asymmetry but E_R^* has reverse skewness. Also, there is not a large difference between the frequencies corresponding to the maxima of E_R^* and E_G^* , suggesting that in fact a single relaxation process is operative and therefore that decomposition into two relaxations is artificial.

Finally, the assumption of simple additivity both of moduli and of strain optical coefficients in (1) and (2) appears to be contradictory. Additivity of components of birefringence would imply additivity of strain (and compliance) rather than stress.

The data are analysed below in terms of a single transition, using a method which avoids additional assumptions such as frequency-temperature superposition.

B. FSSM analysis of complex modulus

Following the method applied previously [8] in another case of failure of time-temperature superposition, the FSSM was adjusted to the data of Figs 1 and 2 independently at each temperature. Because of data scatter and the narrow frequency range explored, meaningful parameters could not easily be obtained from the Cole-Cole plots. These plots were used, however, to obtain starting values for β and E_G , ΔE or E_r at low, intermediate and high temperatures respectively. Remaining parameters were then obtained from the frequency dependence of storage and loss modulus. At

each step, adjustable parameters were chosen so as to minimize interdependence of parameters. For instance, at low temperatures E'' is sensitive to K and β , but not to ΔE . Including ΔE among the adjustable parameters leads to dependencies close to 100% and to unrealistic parameters. Best-fit parameter sets obtained from E' and E'' usually differ. The procedure is iterated until reasonable convergence. Parameters obtained as averages of best-fit values from E' and E'' are given in Table I. The parameters of the spring-pot are expressed here in terms of τ (rather than K) and β : in view of the temperature dependence of β , K has temperature-dependent dimensions. At the lowest temperatures results were insensitive to E_r , which was set arbitrarily at 8 MPa which is approximately the average of values obtained at higher temperatures.

Difficulties in obtaining a single set of parameters affording a good description of both loss and storage modulus could be an indication that the four-parameter fractional Zener model is oversimplified. However, it has been shown recently [12] that the presence of the slowly-decaying transient typical of long-memory materials is liable to induce frequency-dependent errors in DMTA measurements, leading to difficulties in retrieving true material parameters from DMTA or other dynamic measurements. As there is no indication of complexity in the glass transition range in polycarbonate, no improvement was expected from increasing the number of material parameters.

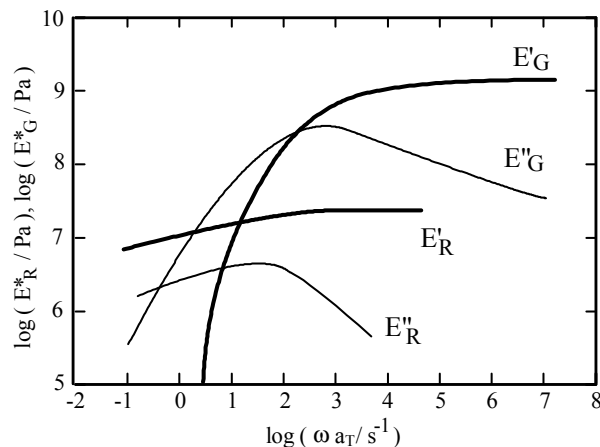


Fig. 7. Master curves of component functions E_R^* and E_G^* (schematic, after Hwang et al. [1])

The curves on Figs. 1 and 2 are calculated from (5) using the parameters given in table I. Thus the simplest form of FSSM is seen to be quite adequate to describe the complex modulus of polycarbonate in its glass transition range. Deviations at low frequency at the highest temperature (170°C) can be attributed to the approaching terminal transition to viscous flow, which is not taken into account by the FSSM model of Fig. 5.

The temperature dependence of best fit parameters is as expected: the decrease of E_u can be attributed to thermal expansion which weakens the van der Waals forces responsible for the glassy modulus. The near-constancy of E_r at the highest temperatures can be attributed to two partially

compensating effects. At constant conformation, the rubbery modulus is expected to be proportional to absolute temperature. However the entanglement length increases with temperature due to an increase in *cis* conformations of the carbonate submolecule, which are energetically less favourable than *trans*: the decrease of entanglement length for extended conformations and vice-versa is well established for flexible polymer chains [13]. An increase of β with temperature is to be expected: values close to 1 are a token of absence of cooperativity. Higher cooperativity is required for molecular motions to occur at lower temperatures. At the highest temperature the fit is clearly less good: because of the approach of the terminal transition to viscous flow, a simple FSSM involving a single spring-pot is no longer adequate. Although an improved model accounting for the terminal transition has been successfully applied previously, this was not attempted here because the discrepancy is only perceptible at a single temperature.

C. FSSM analysis of complex SNOC

To interpret SNOC behaviour, it was first attempted to obtain the required dependence directly from the FSSM model of Fig. 5, assuming birefringence to be the sum of two contributions, one proportional to stress (i.e. to strain of E_0) and the other to retarded strain (i.e. strain of the Voigt element or of E_1). It was found impossible to obtain an appropriate fit by this method, essentially because according to this procedure the time constant is identical for modulus and for SNOC, whereas the experimental maxima of O'' and of E'' occur at different frequencies.

TABLE I
FSSM PARAMETERS FOR MODULUS

T	E_u (GPa)	E_r (MPa)	τ (s)	β
148	1.52	(8)	57	0.29
150	1.45	(8)	2.0	0.41
152	1.38	(8)	0.314	0.49
154	1.31	(8)	0.078	0.55
156	1.12	(8)	0.025	0.64
158	1.03	10	7.0e-3	0.70
160	0.83	9.2	2.5e-3	0.78
163	0.60	7.32	1.0e-3	0.86
166	0.58	7.5	2.7e-4	0.86
170	0.56	7.5	5.5e-5	0.86

It was then attempted to analyse the strain-optical coefficient using (8), independently from the fit of E'' although following a similar procedure, yielding the parameters of table II. It was found that a background contribution to O'' was required to obtain a reasonable fit.

This background, denoted O_{bk} was assumed to be independent of frequency but was allowed to vary with temperature. Again, at the lowest temperatures the fit was insensitive to O_r which was set at a constant arbitrary value obtained by extrapolation from higher temperatures.

Comparison of tables I and II shows that although the temperature variation of τ is similar for modulus and for strain-optical coefficient, the latter τ is systematically larger

than the former. This is illustrated on Fig. 8. Also, the β values are similar at low temperatures but differ in the upper range of investigated temperatures: they reach a lower asymptotic value, at a lower temperature, for the strain-optical coefficient than for the complex modulus. Both observations tell us that birefringence is related to molecular motions on a larger length scale than those responsible for frequency and temperature dependence of modulus.

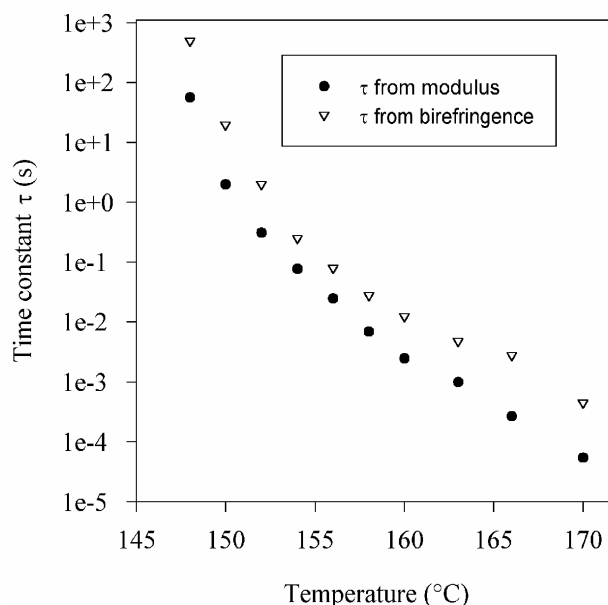


Fig. 8. Temperature dependence of time constants for modulus and birefringence of polycarbonate

TABLE II
FSSM PARAMETERS FOR BIREFRINGENCE

T	O_u	O_r	τ (s)	β	O_{bk}
148	0.168	(0.07)	500	0.29	5e-4
150	0.162	(0.07)	20	0.41	1e-3
152	0.159	(0.07)	2	0.49	1.5e-3
154	0.158	(0.07)	0.25	0.58	2.5e-3
156	0.154	0.062	0.08	0.62	3e-3
158	0.142	0.06	0.028	0.65	4.6e-3
160	0.137	0.052	0.013	0.67	4.2e-3
163	0.13	0.045	4.8e-3	0.66	4.5e-3
166	0.12	0.038	2.8e-3	0.65	3.5e-3
170	0.12	0.038	4.5e-4	0.65	5e-3

Such behaviour is not unusual in polymers. It was found previously [14] that the time to reach steady state in the annealing range in polycarbonate (i.e. approximately T_g to $T_g-25^\circ\text{C}$) was longer for enthalpy relaxation measured in DSC than for conformational relaxation observed in IR spectroscopy or for volume relaxation. Thus even though a single relaxation process is active in the glass transition range, this process expresses itself through different exponents and characteristic times according to the observed physical property.

V CONCLUSIONS

The Fractional Standard Solid Model has been shown previously to be particularly well suited to description of polymer viscoelasticity in the linear range. It has been shown here to afford also an excellent description of dynamic birefringence. Such models allow a good description of behaviour using a minimal number of parameters, and allow meaningful parameters to be obtained without introducing restrictive assumptions. The different temperature dependence of time constants from modulus and from birefringence observed here affords insight into length scales of molecular mobility. This length scale is larger for dynamic birefringence than for modulus. This can be understood as an expression of the fact that the entanglement length is not well defined, but depends on the property under observation.

Discrepancies between parameter sets obtained from storage and loss moduli may be attributed to oversimplification of the model, but alternatively could be a consequence of the slowly decaying transient in dynamic measurements on long-memory materials. This point requires further investigation.

VI. REFERENCES

- [1] E.J. Hwang, T. Inoue and K Osaki, "Viscoelasticity and birefringence of bisphenol A polycarbonate", *Polymer* vol. 34, 1993, pp. 1661-1666.
- [2] H. Okamoto, T. Inoue and K Osaki, "Viscoelasticity and birefringence of Polyisoprene", *J.Polym.Sci. part B : Polymer Physics* vol 33, 1995, pp. 417-424.
- [3] H. Okamoto, T. Inoue and K Osaki, "Viscoelasticity and birefringence of Polyisobutylene", *J.Polym.Sci. part B : Polymer Physics* vol. 33, 1995, pp. 1409-1416.
- [4] T. Inoue, E.J. Hwang and K Osaki, "Birefringence of amorphous polyarylates : 2. Dynamic measurement on a polyarylate with low optical anisotropy." *Polymer* vol. 38, 1997, pp. 1029-1034.
- [5] Watanabe H. and Inoue T., "Conformational dynamics of Rouse chains during creep/recovery processes : a review." *J.Phys : Condens ; Matter* vol. 17, 2005, pp. R607-R636.
- [6] N. Heymans and J.-C. Bauwens, "Fractal rheological models and fractional differential equations for viscoelastic behaviour", *Rheologica Acta*, vol. 33, 1994, pp. 210-219.
- [7] N. Heymans, "Hierarchical models for viscoelasticity : dynamic behaviour in the linear range", *Rheologica Acta*, vol. 35, 1996, pp. 508-519.
- [8] N. Heymans, "Constitutive equations for polymer viscoelasticity derived from hierarchical models in cases of failure of time-temperature superposition", *Signal Processing*, vol 83, 2003, pp. 2345-2357.
- [9] N. Heymans, "On orientational and distortional contributions to birefringence", *J.Polym.Sci.: Part B: Polym. Phys.* vol. 29, 1991, pp. 1193-1201.
- [10] N. Heymans, "Interaction between contributions to birefringence from distortion and orientation in preoriented polycarbonate", *Colloid Polym. Sci.*, vol. 270, 1992, pp. 446-454.
- [11] N. Heymans, "Development of orientation in glassy polycarbonate at high strains", *Polymer*, vol 28, November 1987, pp 2009-2017.
- [12] N. Heymans, "Fractional calculus description of DMTA transient in long-memory materials", *IFAC-FDA06 2nd IFAC workshop on Fractional Differentiation and its Applications*", Porto 19-21 July 2006.
- [13] N. Heymans, "A Novel Look at Models for Polymer Entanglement", *Macromolecules*, vol. 33, 2000, pp. 4226-4234.
- [14] N. Heymans and B. Dequenne, "Relationship between conformation and enthalpy or volume relaxation in polycarbonate", *Polymer*, vol.42, 2001, pp. 5337-5342.